HHS Public Access

Author manuscript

Vascul Pharmacol. Author manuscript; available in PMC 2024 December 01.

Published in final edited form as:

Vascul Pharmacol. 2023 December ; 153: 107235. doi:10.1016/j.vph.2023.107235.

Global and endothelial G-protein coupled receptor 75 (GPR75) knockout relaxes pulmonary artery and mitigates hypoxia-induced pulmonary hypertension

Catherine A. D'Addario[1], **Shun Matsumura**[1], **Atsushi Kitagawa**[1], **Gregg M. Lainer**[2], **Frank Zhang**[1], **Melinee D'silva**[1], **Mohammad Y. Khan**[1], **Ghezal Froogh**[1], **Artiom Gruzdev**[3], **Darryl C. Zeldin**[3], **Michal L. Schwartzman**[1], **Sachin A. Gupte**[1,*]

[1]Department of Pharmacology, New York Medical College, Valhalla, NY, USA 10595

[2]Department of Cardiology, and Heart and Vascular Institute, Westchester Medical Center and New York Medical College, Valhalla, NY, USA 10595

[3]National Institute of Environmental Health Sciences, National Institutes of Health, Research Triangle Park, NC, USA, 27709

Abstract

Rationale: Pulmonary hypertension (PH) is a multifactorial disease with a poor prognosis and inadequate treatment options. We found two-fold higher expression of the orphan G-Protein Coupled Receptor 75 (GPR75) in leukocytes and pulmonary arterial smooth muscle cells from idiopathic PH patients and from lungs of C57BL/6 mice exposed to hypoxia. We therefore postulated that GPR75 signaling is critical to the pathogenesis of PH.

Methods: To test this hypothesis, we exposed global (*Gpr75*$^{-/-}$) and endothelial cell (EC) GPR75 knockout (EC-*Gpr75*$^{-/-}$) mice and wild-type (control) mice to hypoxia (10% oxygen) or normal atmospheric oxygen for 5 weeks. We then recorded echocardiograms and performed right heart catheterizations.

Results: Chronic hypoxia increased right ventricular systolic and diastolic pressures in wildtype mice but not *Gpr75*$^{-/-}$ or EC-*Gpr75*$^{-/-}$ mice. *In situ* hybridization and qPCR results revealed

*Address Correspondence: Sachin A. Gupte, MD, PhD, Professor of Pharmacology, BSB Rm #546, New York Medical College, 15 Dana Road, Valhalla, NY, USA 10595, Tel: 914-594-3937, s_gupte@nymc.edu.

Authors statement:

Catherine A. D'Addario: Performed experiments and contributed analyze the data and write the paper.
Shun Matsumura and Atsushi Kitagawa: Performed cardiac catheterization.
Gregg M. Lainer: Provide human blood samples.
Frank Zhang: Performed wire myography.
Melinee D'silva and Mohammad Y. Khan: Designed probes and performed RNA scope.
Ghezal Froogh: Generated EC-deletion of GPR75.
Artiom Gruzdev and Darryl C. Zeldin: Designed and generated GPR75 KO mice.
Michal L. Schwartzman: Contributed to design experiments in KO mice and advised regarding GPR75 role.
Sachin A. Gupte: Designed experimental concept, analyzed and interpreted the results, and wrote the paper.

Conflict of Interest

None

that *Gpr75* expression was increased in the alveoli, airways and pulmonary arteries of mice exposed to hypoxia. In addition, levels of chemokine (C-C motif) ligand 5 (CCL5), a low affinity ligand of GPR75, were increased in the lungs of wild-type, but not *Gpr75*$^{-/-}$, mice exposed to hypoxia, and CCL5 enhanced hypoxia-induced contraction of intra-lobar pulmonary arteries in a GPR75-dependent manner. *Gpr75* knockout also increased pulmonary cAMP levels and decreased contraction of intra-lobar pulmonary arteries evoked by endothelin-1 or U46619 in cAMP-protein kinase A-dependent manner.

Conclusion: These results suggest GPR75 has a significant role in the development of hypoxia-induced PH.

Graphical Abstract

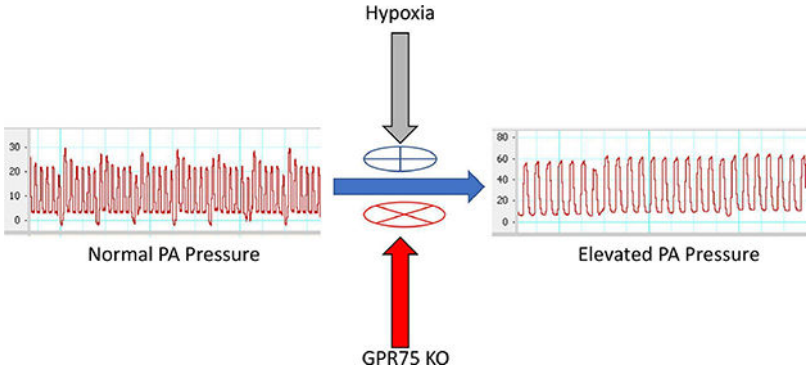

Endothelial dysfunction, increased contraction of smooth muscle cells (SMCs), and pulmonary artery remodeling are the main causes of pulmonary hypertension (PH) – a lung disease with a poor prognosis and inadequate treatment options (1). It is now apparent that elevated levels of various cytokines and chemokines, including chemokine (C-C motif) ligand 5 (CCL5), contribute to the abnormal pulmonary vascular cell growth and function seen in some forms of PH, including hypoxia-induced PH, in both patients and experimental animal models (2, 3). However, very little is known about the role of cytokine/chemokine-related receptor signaling in the pathogenesis of PH. A better understanding of the related cytokine and chemokine signaling that elicits inflammation and promotes pulmonary arterial remodeling, will be useful for developing novel approaches to the treatment of PH.

Chemokines, including CCL5, activate chemotaxis and induce T cell proliferation (4). CCL5 interacts with cells and signals through several G-protein coupled receptors (CCR1, CCR3 and CCR5). In addition, it was recently proposed that CCL5 is a ligand for orphan G-protein coupled receptor 75 (GPR75) in neuronal cells (5). The mRNA encoding GPR75 has been detected in mouse heart, brain, skeletal muscle, liver, kidney, spleen, lungs and testis (5) as well as in vascular endothelial cells (ECs) and SMCs (6). *Gpr75* was originally cloned and characterized from human chromosome 2p16 and was detected in the human retina, retinal arterioles and brain (7). The receptor was subsequently linked to age-related macular degeneration (8), diabetes (9), multiple sclerosis (10), neuroprotection (11), hypertension (6) and obesity (12). Intriguingly, *Gpr75* is also associated with metastatic features of androgen-insensitive prostate cancer cells (13), colorectal neoplasia (14) and lung squamous cell carcinoma (15). However, the precise roles of GPR75 in most of these diseases have not

been experimentally demonstrated, and details of GPR75-associated intracellular signaling remains unclear.

CCL5 and 20-hydroxyeicosatetraenoic acid (20-HETE), low- and high-affinity ligands for GPR75 (16), activate $G_{q\alpha}$ signaling in neuronal cells, ECs and SMCs (5, 6, 11). Acting via GPR75-$G_{q\alpha}$, CCL5 and 20-HETE respectively induce increases in inositol-1,3,5 triphosphate (IP3) and intracellular Ca^{2+} in: 1) a hippocampal cell line, where it is protective against the neurotoxicity of amyloid-β peptide (5), and 2) SMCs, where it appears to enhance phenylephrine-induced contractions and hypertension in mice (6). In addition, CCL5 and 20-HETE are proinflammatory molecules (17, 18). CCL5, which is elevated in PH (2), plays a critical role in T cell activation and proliferation (4), while 20-HETE, a metabolite of arachidonic acid produced by pulmonary arteries in response to hypoxia (19), elicits transient pulmonary arterial contraction followed by relaxation (20). We therefore postulated that GPR75 signaling is crucially involved in PH. To test that idea, we used of a new *Gpr75* knockout mouse model to determine the role of GPR75 in chronic hypoxia-induced PH. The results presented in this study demonstrate, for the first time, that both global and EC GPR75 knockout completely abolish hypoxia-induced contraction of isolated intra-lobar pulmonary arteries (IPAs) and hypoxia-induced PH. These results suggest GPR75 is a major contributor to both lung physiology and pathophysiology and may play significant roles in such lung diseases as focal pneumonia or atelectasis and high-altitude sickness.

Materials and Methods

For detailed descriptions of the methods, refer to the online supplement.

Drugs and reagents:

All chemicals and reagents were purchased from Sigma, Thermo-Fisher, R&D Systems, My BioSource or VWR.

Gpr75 knockout mice:

The conditional null ("Flox") *Gpr75* locus was generated by CRISPR/Cas9-mediated targeting in G4 (B6129F1) embryonic stem (ES) cells (Supplemental Figure 1). The *LoxP* sites flank 3133 bp, which contains 184 bp of introns 1–2, the single coding exon of *Gpr75* (exon 2), the entire 3' UTR, and 208 bp of the 3' extragenic sequence (floxed sequence chr11:30,890,805–30,893,937 [GRCm38/mm10]). CAS9 double stranded breaks were targeted to CAGGAATACGACCTCTCCATNGG (5') and CCAAAATCCTATACTAGTAGNGG (3') using the PX459v2 SgRNA/CAS9/Puro delivery plasmid, a gift from Feng Zhang (21). Two circular repair templates, each with 600 bp total homology, were used to insert the *LoxP* sites. To aid clonal screening, a unique restriction endonuclease site was inserted with each *LoxP* site: BamHI (5' *LoxP*) and ClaI (3' *LoxP*). ES clonal screening was done with high fidelity PCR, which was followed by restriction digestion and was confirmed by direct sequencing of the PCR amplicon and sequencing verification with the PCR primers (5' LoxP-Fwd: GTACATTGTGCACCTCTTCACAC; 5' LoxP-Rev: CTTCCTGAAGGATGGGTCAAAGA; 3' LoxP-Fwd: ACCAAGCTGTTACAAATGTGCTG; and 3' LoxP-Rev:

TTGGTTGCTTAATATGCATGACCC). To confirm that no aberrant recombination occurred within the *Gpr75* coding exon, the entire targeted locus was PCR amplified and sequenced using the distal screening primers (5'LoxP-Fwd and 3' LoxP-Rev). Neither of the two CAS9 target sequences were predicted to have any genetically linked off-target sites; therefore, the ES clones were not screened for any off-target CAS9-mediated mutations.

Homozygously targeted ES clones were microinjected into wildtype blastocysts for standard chimeric founder generation. The primary *Gpr75* flox allele was maintained as a perpetual backcross to wild-type C57BL/6J mice. To generate the *Gpr75*-deficient allele, the *Gpr75* flox allele was crossed to B6 CMV-Cre transgenic mice [Jackson Labs Strain 006054; (22)]. Cre-mediated recombination/excision of the floxed genomic region was confirmed by direct amplicon sequencing. To generate EC-*Gpr75* knockout, we crossed the *Gpr75* flox mice with non-inducible Tie2-Cre transgenic mice purchase from Jackson laboratory. Genotyping of the flox and null mouse colonies was done by Transnetyx using allele-specific primer/probe assays. Because PH is multicellular disease, we chose to use global and EC GPR75 knockout mice to characterize the role of GPR75 signaling in its pathogenesis.

Animal models and experimental protocols:

All animal experiments were approved by the New York Medical College Animal Care and Use Committee, and all procedures conformed to the guidelines from the NIH Guide for the Care and Use of Laboratory Animals. Global and EC $Gpr75^{-/-}$ male and female mice (15–18 g) and age-matched wild-type mice (15–18 g; controls/littermates) were randomly divided into normoxia (Nx) and hypoxia (Hx) groups. Mice in the Nx group were placed in a normoxic (21% O_2) environment, while the Hx group was placed in a normobaric hypoxic chamber (10% O_2) for 5 weeks. Hx mice are a preclinical model of PH (23). At the end of the treatment period, hemodynamic measurements were performed, tissues (lungs, hearts, and arteries) were harvested, and blood samples were collected.

Lungs were isolated as described previously (24) and according to the recommendations of the American Thoracic Society (25). Briefly, we inflated the left lung lobes with 0.5% agarose in 1% neutral buffered formalin at 20 cmH_2O pressure and then fixed the tissue in 10% neutral buffered formalin overnight (24). We then embedded the formalin-fixed lung in paraffin and cut 5-μm sections, which were stained with H&E, Mason's Trichrome and Verhoeff Van Gieson stain to evaluate pulmonary arterial remodeling. Remodeling of small (< 50 μm), medium (50–100 μm) and large (>100 μm) pulmonary arteries was assessed using the Heath-Edward grading system, as previously described (24, 26).

Collection of blood from control individuals and PH patients:

Protocols were approved by the New York Medical College and Westchester Medical Center IRB. Written consent was obtained from all participants before blood was collected, after which leukocytes were isolated from scleroderma and idiopathic pulmonary hypertensive patients as well as from control individuals. Patients' demographic and hemodynamic characteristics were presented in our earlier publication (27). In the present study, we used left over total mRNA to assess *Gpr75* expression.

Statistical analysis:

Statistical analysis was performed using GraphPad Prism 7.0e software. Values are presented as the mean ± standard error (SE). Statistical comparisons of samples were performed with two-way ANOVA followed by Fisher's LSD post hoc test. Student's t test was used to compare the two groups. Differences with $P<0.05$ between the groups was considered significant.

Results:

CCL5 levels and *GPR75* expression are increased in PH:

Recent studies have shown that immunogenic/inflammatory cells and stem cells recruited from the circulation to the lungs contribute to the increase in the inflammatory cytokine gradient around the pulmonary arteries and to the pathogenesis of PH (27, 28). Therefore, to determine whether GPR75 and its putative ligands, CCL5 and 20-HETE, are increased in PH patients, we measured expression of *GPR75* mRNA in leukocytes and levels of CCL5 and 20-HETE in plasma from patients with scleroderma-associated or idiopathic PH (Figure 1). *GPR75* expression was higher in leukocytes from PH patients than in those from control individuals (Figure 1A). CCL5 levels were higher ($P<0.05$) in plasma from PH patients than from controls (Figure 1B), whereas plasma 20-HETE levels did not differ between the PH patients and controls (Figure 1C).

CCL5 and *Gpr75* expression increases and 20-HETE decreases in lungs of mice exposed to hypoxia:

To determine whether GPR75, CCL5 and/or 20-HETE are increased in experimental models of PH, we measured *Gpr75* expression and CCL5 and 20-HETE levels in lungs from wild-type mice exposed to hypoxia (Hx) or normoxia (Nx) for 5 weeks. As anticipated, *Gpr75* expression was higher in lungs from Hx than Nx mice (Figure 1D), as were CCL5 levels (Figure 1E). By contrast, 20-HETE levels were lower in lungs from Hx mice than Nx mice (Figure 1F).

Gpr75 expression is increased in lungs from wild-type mice exposed to hypoxia:

Because *Gpr75* mRNA levels were increased in PH patients and Hx mice, we employed RNAscope (*in situ* hybridization) to assess expression of *Gpr75* in mouse lungs because commercially available antibodies are non-specific. Our results revealed *Gpr75* mRNA signals (red) in and around alveoli, airways, and pulmonary arteries [identified by yellow von Willibrand factor (vWF) staining for endothelial cells] in wild-type Nx and Hx mice (Fig. 2A). However, the signals were much stronger in the lungs of Hx mice. By contrast, little or no *Gpr75* signal was detected in the lungs of $Gpr75^{-/-}$-Hx mice (Fig. 2A). Real-time PCR results showed the presence of *Gpr75* mRNA in the lungs and heart from wild-type mice but not $Gpr75^{-/-}$ mice (Figure 2B and 2C). Moreover, *Gpr75* mRNA levels were increased in the lungs of wild-type Hx mice but not $Gpr75^{-/-}$-Hx mice (Figure 2B). Interestingly, cardiac levels of *Gpr75* mRNA were decreased in wild-type Hx mice (Figure 2C).

CCL5 is increased in lungs from wild-type mice and requires GPR75 to elicit contraction of isolated IPAs:

Increases in inflammatory chemokines contribute to the pathogenic remodeling of pulmonary arteries in PH patients and animal models (1, 2, 29). CCL5, a proinflammatory chemokine, has been implicated in pulmonary arterial remodeling and shown to elicit contraction of saphenous vein and coronary artery (30). Because CCL5 is a low-affinity ligand for GPR75 (16), we tested whether CCL5-GPR75 signaling contributes to pulmonary arterial contractility. As compared to the corresponding Nx mice, *Ccl5* expression was higher in lungs from wild-type Hx mice but not *Gpr75*$^{-/-}$-Hx mice (Figure 3A). At the same time, CCL5 levels were increased in wild-type Hx, but not *Gpr75*$^{-/-}$-Hx, mice as compared to the corresponding Nx mice (Figure 3B). We next examined the effect of CCL5 on contractile force in IPAs. Intriguingly, hypoxia-induced contractions in IPAs from *Gpr75*$^{-/-}$ mice were weaker than in those from wild-type mice (Figure 3C). In addition, application of CCL5 (1 ng/ml) to IPAs from wild-type mice enhanced the second phase of hypoxia-induced contractions (Figure 3C).

Gpr75 knockout increases cAMP levels and decreases IPA contractility via cAMP-protein kinase A-dependent signaling:

Earlier studies showed that GPR75 activates $G_{q\alpha}$ and $G_{\alpha i}$ signaling (5, 31, 32). Therefore, to investigate the GPR75-dependent signaling that regulates pulmonary arterial contractility, we measured levels of $G_{q\alpha}$- and $G_{\alpha i}$-associated second messengers (IP3 and cAMP, respectively) in lungs from *Gpr75*$^{-/-}$ and wild-type mice. Interestingly, while IP3 levels did not differ between lungs from *Gpr75*$^{-/-}$ and wild-type mice (Figure 4A), cAMP levels were five-fold higher in the lungs of *Gpr75*$^{-/-}$ than wild-type mice (Figure 4B). Then to determine whether CCL5-GPR75 pairing decreases cAMP, we measured cAMP levels in lung tissue from *Gpr75*$^{-/-}$ and wild-type mice incubated with CCL5 (1 ng/ml). Application of CCL5 to lungs from wild-type mice, but not *Gpr75*$^{-/-}$ mice, significantly reduced cAMP levels (Supplement Table 1). Therefore, given that cAMP reduces intracellular Ca^{2+} and relaxes smooth muscle, we assessed the effect of elevated cAMP on the contractility of IPAs from wild-type and *Gpr75*$^{-/-}$ mice. We first tested the response to KCl, which elicits SMC contractions by activating Ca^{2+} influx through voltage-gated Ca^{2+} channels as well as by activating a Rho kinase-mediated pathway (33). We found that IPAs from *Grp75*$^{-/-}$ mice exhibited weaker KCl-induced contractions than those from wild-type mice (Figure 4C). We then tested the response of IPAs to ZD7288, a cAMP-gated ion channel inhibitor, and found that ZD7288 elicited stronger IPA contractions in wild-type than *Gpr75*$^{-/-}$ mice (Figure 4D). Elevated levels of thromboxane and endothelin-1 have also been implicated in hypoxia-induced pulmonary contraction and in the pathogenesis of various forms of PH (34). Interestingly, contractions elicited by U46619, a thromboxane analogue, or endothelin-1 in IPAs from *Gpr75*$^{-/-}$ mice were weaker than those elicited in IPAs from wildtype mice (Figure 4E and F).

It is well established that cAMP stimulates protein kinase A (PKA) signaling, which decreases SMC contraction by reducing 1] Ca^{2+} influx through ion channels, 2] intracellular Ca^{2+} levels by inhibiting Ca^{2+} release from internal stores or by accelerating Ca^{2+} uptake into the SR, and 3] Ca^{2+} sensitivity to the myofilaments. Therefore, to determine whether

GPR75-cAMP signaling affects tonic or sustained contraction of IPA, we tested the effects of 8-Br-cAMP (10 μM), a PKA activator, and Rp-cAMPs (10 μM), a PKA inhibitor, on IPA contractions evoked by KCl (60 mM) and endothelin-1 (1 μM) in a time dependent manner. In response to KCl or endothelin-1, IPAs isolated from wild-type mice and pretreated with 8-Br-cAMP exhibited weaker contractions while those pretreated with Rp-cAMPs exhibited stronger contractions than unpretreated vessels (Figure 5A and B). By contrast, IPAs isolated from *Gpr75*$^{-/-}$ mice was refractory to the effects of 8-Br-cAMP on KCl- and endothelin-1-evoked contractions and even enhanced contractions evoked by KCl (Figure 5C and D). Moreover, IPAs from *Gpr75*$^{-/-}$ mice pretreated with Rp-cAMPs contracted more gradually (Figure 5C and D) than those from wild-type mice (within 5 mins) in response to KCl or endothelin-1 (Figure 5A and B).

Gpr75 knockout decreases hypoxia-induced right ventricular pressure and hypertrophy but not pulmonary arterial remodeling:

Because *Gpr75* knockout upregulated cAMP and decreased the contribution of CCL5-GPR75 to hypoxia-induced pulmonary artery contraction, our next goal was to determine the role of GPR75 in mediating chronic hypoxia-induced PH. Chronic hypoxia (for 5 weeks) increased right ventricular pressure (Figure 6A, B and C) and hypertrophy (Figure 6D) in wild-type mice but not *Gpr75*$^{-/-}$ mice. Furthermore, the PAAT-to-ET ratio, left ventricular diameter (LVD), left ventricular volume (LVV), fraction shortening (FS), stroke volume (SV), stroke work (SW), ejection faction (EF) and cardiac index (CI) were all higher in *Gpr75*$^{-/-}$-Hx than wild-type Hx mice (Supplement Table 2 and 3). Intriguingly, right ventricular diastolic pressure was lower and PApeakV was higher in *Gpr75*$^{-/-}$-Nx mice than wild-type Nx mice (Figure 6C and Supplement Table 2). Verhoeff Van Gieson staining (Figure 6E) showed the pulmonary artery remodeling (medial hypertrophy or wall thickness determined from the internal and external lamina) does not appear to differ between the experimental groups (Figure 6F).

EC-*Gpr75* knockout decreases hypoxia-induced right ventricular pressure:

Because *Gpr75* expression was 50% higher in human pulmonary artery ECs than SMCs (Supplement Table 4), we generated EC-*Gpr75*$^{-/-}$ mice to determine the importance of EC-GPR75 in the pathogenesis of hypoxia-induced PH. We validated EC knockout by measuring *Gpr75* mRNA in CD-31 enriched ECs isolated from lungs (Figure 7A and B). Interestingly, EC-*Gpr75* knockout reduced the hypoxia-induced increase of right ventricular systolic and diastolic pressures (Figure 7C, D, E), and the reduction in pressure was comparable to that observed in global *Gpr75*$^{-/-}$ mice (Figure 6B and C).

Discussion

The results of this study provide the first experimental evidence that GPR75 receptor signaling contributes to the pathogenesis PH in mammals, as global and EC knockout of *Gpr75* in mice weakened hypoxia-induced contraction of IPAs and reduced right ventricular pressure. We therefore propose that GPR75 signaling is critical to both lung physiology and pathophysiology.

Using *in situ* hybridization, *Gpr75* signals were detected in arteries, airways, and alveoli in mouse lungs. GPR75 express more in mouse ECs than SMCs (6). Consistent with that finding, *GPR75* was expressed in cultured human pulmonary artery ECs more than SMCs. Notably, Expression of *GPR75* mRNA was 2-fold higher in leukocytes from patients with scleroderma-associated or idiopathic PH than in those from control subjects and was three-fold higher in lungs from wild-type Hx mice than in lungs from Nx mice. This suggests *Gpr75* expression is sensitive to changes in O_2 tension and increased GPR75 levels could potentially play a role in the initiation and/or maintenance of PH. Our finding that global or EC *Gpr75* knockout prevented hypoxia-induced increases in right ventricular pressure and hypertrophy indicates that GPR75 signaling contributes to increased afterload on the right heart in response to sustained hypoxia-induced pulmonary artery contraction. Increased contraction and remodeling of large and small pulmonary arteries impede blood flow through the lungs and increase afterload on the right heart (1). In mice, unlike in rats, pulmonary artery contraction and remodeling equally contribute to the development of hypoxia-induced PH (35). Because *Gpr75* knockout reduced RVSP but not pulmonary artery hypertrophy, we suggest remodeled (thicker) pulmonary arteries in the hypoxic lungs from *Gpr75*$^{-/-}$ mice impaired blood flow during systole. Additionally, *Gpr75* knockout decreased the second phase of hypoxia-induced contraction of IPAs. These findings suggest that increased *Gpr75* transcription and GPR75 receptor-dependent signaling contributes to a setting in which pulmonary arteries are constricted and right ventricular pressure is increased in mice exposed to chronic hypoxia.

We next sought to determine the signaling that relieved the hypoxia-induced increase in right ventricular pressure in *Gpr75*$^{-/-}$ mice. Because recent studies suggest GPR75 mediates $G_{q\alpha}$ signaling (5), we anticipated that *Gpr75* knockout would decrease pulmonary IP3 levels. Unexpectedly, our findings revealed that *Gpr75* knockout led to a >5-fold increase in cAMP levels, which is regulated by G_s- and $G_{\alpha i}$-dependent signaling, without affecting IP3 levels in lungs of Nx mice. Although these findings seem paradoxical, they are not unprecedented. Two recent studies showed that overexpression of GPR75 reduces cAMP in cultured cells (31, 32). Given that *Gpr75* knockout decreased pulmonary GPR75 mRNA signals, we suggest that cAMP was increased in all cell types within those airways and pulmonary vasculature. Collectively then, our findings with *Gpr75*$^{-/-}$ mice together with results from earlier GPR75 overexpression studies suggest GPR75 associates with $G_{\alpha i}$-coupled receptor signaling.

It is well established that cAMP signaling robustly elicits relaxation of SMCs and dilation of blood vessels, including pulmonary arteries, by: 1] decreasing Ca^{2+} influx through voltage-gated and store-operated Ca^{2+} channels (1, 36), 2] increasing Ca^{2+} uptake and sequestration by the sarcoplasmic reticulum (37, 38), and 3] decreasing the Ca^{2+} sensitivity of myofilaments (39). Hypoxia increases intracellular Ca^{2+} and enhances the Ca^{2+} sensitivity to myofilaments in SMCs and thus elicits pulmonary artery contraction (40). In that regard, IPAs from *Gpr75*$^{-/-}$ mice contracted less than those from wild-type mice in response to 1] hypoxia; 2] U46619 (a thromboxane analogue) and endothelin-1, two mediators of pulmonary hypertension; 3] KCl, a membrane depolarizing agent; and 4] a cyclic nucleotide (cAMP)-gated ion channel inhibitor. These results indicate that activation of cAMP-PKA signaling would likely reduce force generation in IPAs from *Gpr75*$^{-/-}$ mice

in response to various contractile agents. This was confirmed by our results showing that IPAs from wildtype mice, but not *Gpr75*$^{-/-}$ mice, contracted less to KCl or endothelin-1 when pretreated with a PKA activator. These observations therefore suggest that IPAs from *Gpr75*$^{-/-}$ mice, which had five-fold higher cAMP levels, were refractory to the cAMP analogue and paradoxically contracted more in the presence of KCl, which evokes SMC contraction by activating Ca^{2+} influx through voltage-gated Ca^{2+} channels as well as by activating Rho kinase-mediated pathway (33). At the same time, IPAs from *Gpr75*$^{-/-}$ mice pretreated with a PKA inhibitor only gradually contracted, suggesting it took longer for the inhibitor to competitively inhibit PKA signaling in IPAs from *Gpr75*$^{-/-}$ than wild-type mice. Intracellular as well as secreted cAMP-dependent signaling inhibits SMC contraction and mitigates PH (41). In addition, cAMP signaling controls cell proliferation, migration, and gene expression (42, 43). We therefore propose that the elevated cAMP in *Gpr75*$^{-/-}$ mice acted to dilate the pulmonary circulation and mitigate PH.

Elevated levels of chemokines, including CCL5, contribute to unresolved inflammation and remodeling of pulmonary arteries in the lungs of PH patients and animal models (1, 2). CCL5 has been detected in NK-cells, T and B cells, mast cells, macrophages, ECs, and SMCs in lungs. As expected, lungs from wild-type Hx mice expressed higher levels of CCL5 mRNA and protein than lungs from Nx mice. Interestingly, hypoxia-induced *Ccl5* expression was prevented in the lungs of *Gpr75*$^{-/-}$ mice. Because hemodynamic stress contributes to perivascular inflammation in experimental models of PH (44), we suggest cAMP-mediated relaxation of pulmonary arteries, leading to decreased hemodynamic stress, prevented hypoxia-induced *Ccl5* expression in the lungs of *Gpr75*$^{-/-}$ mice. cAMP signaling represses *Ccl5* in human airway SMCs and cancer cells (45–47), and CREB prevents recruitment of myeloid cells to the adventitia (48). Because *GPR75* is expressed in leukocytes and *Gpr75* knockout blocked the increase in pulmonary *Ccl5*/CCL5 in mice exposed to hypoxia, this also suggests *Gpr75* knockout reduces chemotaxis and recruitment of precursors of immunogenic and proinflammatory cells to the lungs of hypoxic mice. Nonetheless, *Gpr75* knockout did not mitigate pulmonary arterial remodeling (wall thickening/hypertrophy). That suggests reducing CCL5 was either not sufficient to reverse remodeling of the pulmonary artery or CCL5-GPR75 signaling does not contribute to the pathogenesis of the remodeling, and other proinflammatory cytokines/chemokines unaffected by *Gpr75* knockout contribute to its development.

CCL5 and 20-HETE, two proposed GPR75 ligands (5, 6, 16), are proinflammatory molecules as well as vasoconstrictors (17, 18, 49). CCL5 strengthened contraction during the second phase of hypoxia-induced response in IPAs isolated from wild-type mice but not those from *Gpr75*$^{-/-}$ mice. Moreover, the finding that CCL5 significantly decreased cAMP in lung tissue from wild-type mice but not *Gpr75*$^{-/-}$ mice implies that CCL5-GPR75 pairing in conjunction with other CCL5-CCR signaling plays a role in lowering cAMP levels and mediating hypoxia-induced pulmonary contraction. CCL5 has been shown to induced contraction of saphenous vein and coronary artery (30), and we showed here for the first time that CCL5 augments hypoxia-induced pulmonary artery contraction. 20-HETE has been shown to evoke a potent dilatory response in human and rabbit pulmonary vascular and bronchiolar rings (50) and to only transiently contract bovine pulmonary artery (20). We therefore propose that reducing 20-HETE levels in the lungs of wild-type Hx mice

contributed to the enhancing the hypoxia-induced IPA contractions. Normally, hypoxic pulmonary contraction occurs as a homeostatic response to focal pneumonia or atelectasis that adjusts Po_2 without changing pulmonary arterial pressure (51). However, sustained global hypoxic pulmonary contraction, such as occurs at high altitude or with chronic obstruction of an airway, increases pulmonary arterial pressure and initiates PH (51). We therefore suggest that increased CCL5-GPR75 signaling contributes to hypoxia-induced pulmonary arterial contraction and the pathogenesis of PH.

PH is an incurable disease. In the present study, we provide significant evidence that GPR75 signaling, which has been associated with lung squamous cell carcinoma (15), is a novel contributor to the pathogenesis of hypoxia-induced PH in an experimental model. Moreover, our results demonstrate that EC *Gpr75* knockout is sufficient to ameliorate the hypoxia-induced PH. In sum, we propose that GPR75 signaling plays a pivotal role in respiratory physiology and in the pathogenesis of pulmonary diseases. Thus, GPR75 could be a useful new pharmacotherapeutic target for the treatment of pulmonary vascular diseases.

Limitation:

It should be noted that non-inducible Tie2 is expressed in precursor cells in addition to ECs. Therefore, results from this study should be cautiously interpreted in the view of the plausibility that Tie2-Cre driven *Gpr75* gene could be deleted in precursor cells and ECs. Therefore, contribution of precursor cell *Gpr75* knockout to reduce hypoxia-induced PH cannot be eliminated or ignored at this stage. More studies are needed to determine the role EC-specific Gpr75 in mediating PH.

Supplementary Material

Refer to Web version on PubMed Central for supplementary material.

Acknowledgements:

We wish to thank the Shimadzu LC-MS/MS Lipidomic core and Dr. Bellner for his assistance in measuring 20-HETE.

Funding Sources:

This study was supported, in part, by NHLBI (HL139793 to MLS and HL132574 to SAG), the Intramural Research Program of the NIH, National Institute of Environmental Health Sciences grants (Z01ES025034 to DZ), and AHA Grant-in-Aid (17GRNT33670454 to SAG).

References

1. Morrell NW, Adnot S, Archer SL, Dupuis J, Jones PL, MacLean MR, McMurtry IF, Stenmark KR, Thistlethwaite PA, Weissmann N, Yuan JX, Weir EK. Cellular and molecular basis of pulmonary arterial hypertension. J Am Coll Cardiol 2009; 54: S20–31. [PubMed: 19555855]
2. Hassoun PM, Mouthon L, Barbera JA, Eddahibi S, Flores SC, Grimminger F, Jones PL, Maitland ML, Michelakis ED, Morrell NW, Newman JH, Rabinovitch M, Schermuly R, Stenmark KR, Voelkel NF, Yuan JX, Humbert M. Inflammation, growth factors, and pulmonary vascular remodeling. J Am Coll Cardiol 2009; 54: S10–19. [PubMed: 19555853]
3. Frid MG, McKeon BA, Thurman JM, Maron BA, Li M, Zhang H, Kumar S, Sullivan T, Laskowsky J, Fini MA, Hu S, Tuder RM, Gandjeva A, Wilkins MR, Rhodes CJ, Ghataorhe P, Leopold JA, Wang RS, Holers VM, Stenmark KR. Immunoglobulin-driven Complement Activation Regulates

Proinflammatory Remodeling in Pulmonary Hypertension. Am J Respir Crit Care Med 2020; 201: 224–239. [PubMed: 31545648]

4. Bacon KB, Premack BA, Gardner P, Schall TJ. Activation of dual T cell signaling pathways by the chemokine RANTES. Science 1995; 269: 1727–1730. [PubMed: 7569902]
5. Ignatov A, Robert J, Gregory-Evans C, Schaller HC. RANTES stimulates Ca2+ mobilization and inositol trisphosphate (IP3) formation in cells transfected with G protein-coupled receptor 75. Br J Pharmacol 2006; 149: 490–497. [PubMed: 17001303]
6. Garcia V, Gilani A, Shkolnik B, Pandey V, Zhang FF, Dakarapu R, Gandham SK, Reddy NR, Graves JP, Gruzdev A, Zeldin DC, Capdevila JH, Falck JR, Schwartzman ML. 20-HETE Signals Through G-Protein-Coupled Receptor GPR75 (Gq) to Affect Vascular Function and Trigger Hypertension. Circ Res 2017; 120: 1776–1788. [PubMed: 28325781]
7. Tarttelin EE, Kirschner LS, Bellingham J, Baffi J, Taymans SE, Gregory-Evans K, Csaky K, Stratakis CA, Gregory-Evans CY. Cloning and characterization of a novel orphan G-protein-coupled receptor localized to human chromosome 2p16. Biochem Biophys Res Commun 1999; 260: 174–180. [PubMed: 10381362]
8. Sauer CG, White K, Stohr H, Grimm T, Hutchinson A, Bernstein PS, Lewis RA, Simonelli F, Pauleikhoff D, Allikmets R, Weber BH. Evaluation of the G protein coupled receptor-75 (GPR75) in age related macular degeneration. Br J Ophthalmol 2001; 85: 969–975. [PubMed: 11466257]
9. Liu B, Hassan Z, Amisten S, King AJ, Bowe JE, Huang GC, Jones PM, Persaud SJ. The novel chemokine receptor, G-protein-coupled receptor 75, is expressed by islets and is coupled to stimulation of insulin secretion and improved glucose homeostasis. Diabetologia 2013; 56: 2467–2476. [PubMed: 23979485]
10. Alavi MS, Karimi G, Roohbakhsh A. The role of orphan G protein-coupled receptors in the pathophysiology of multiple sclerosis: A review. Life Sci 2019; 224: 33–40. [PubMed: 30904492]
11. Dedoni S, Campbell LA, Harvey BK, Avdoshina V, Mocchetti I. The orphan G-protein-coupled receptor 75 signaling is activated by the chemokine CCL5. J Neurochem 2018; 146: 526–539. [PubMed: 29772059]
12. Akbari P, Gilani A, Sosina O, Kosmicki JA, Khrimian L, Fang YY, Persaud T, Garcia V, Sun D, Li A, Mbatchou J, Locke AE, Benner C, Verweij N, Lin N, Hossain S, Agostinucci K, Pascale JV, Dirice E, Dunn M, Regeneron Genetics C, Discov EHRC, Kraus WE, Shah SH, Chen YI, Rotter JI, Rader DJ, Melander O, Still CD, Mirshahi T, Carey DJ, Berumen-Campos J, Kuri-Morales P, Alegre-Diaz J, Torres JM, Emberson JR, Collins R, Balasubramanian S, Hawes A, Jones M, Zambrowicz B, Murphy AJ, Paulding C, Coppola G, Overton JD, Reid JG, Shuldiner AR, Cantor M, Kang HM, Abecasis GR, Karalis K, Economides AN, Marchini J, Yancopoulos GD, Sleeman MW, Altarejos J, Della Gatta G, Tapia-Conyer R, Schwartzman ML, Baras A, Ferreira MAR, Lotta LA. Sequencing of 640,000 exomes identifies GPR75 variants associated with protection from obesity. Science 2021; 373. [PubMed: 34437096]
13. Cardenas S, Colombero C, Panelo L, Dakarapu R, Falck JR, Costas MA, Nowicki S. GPR75 receptor mediates 20-HETE-signaling and metastatic features of androgen-insensitive prostate cancer cells. Biochim Biophys Acta Mol Cell Biol Lipids 2020; 1865: 158573. [PubMed: 31760076]
14. Ashktorab H, Daremipouran M, Goel A, Varma S, Leavitt R, Sun X, Brim H. DNA methylome profiling identifies novel methylated genes in African American patients with colorectal neoplasia. Epigenetics 2014; 9: 503–512. [PubMed: 24441198]
15. Li Y, Gu J, Xu F, Zhu Q, Ge D, Lu C. Novel methylation-driven genes identified as prognostic indicators for lung squamous cell carcinoma. Am J Transl Res 2019; 11: 1997–2012. [PubMed: 31105813]
16. Pascale JV, Park EJ, Adebesin AM, Falck JR, Schwartzman ML, Garcia V. Uncovering the signalling, structure and function of the 20-HETE-GPR75 pairing: Identifying the chemokine CCL5 as a negative regulator of GPR75. Br J Pharmacol 2021.
17. Nosalski R, Guzik TJ. Perivascular adipose tissue inflammation in vascular disease. Br J Pharmacol 2017; 174: 3496–3513. [PubMed: 28063251]
18. Ishizuka T, Cheng J, Singh H, Vitto MD, Manthati VL, Falck JR, Laniado-Schwartzman M. 20-Hydroxyeicosatetraenoic acid stimulates nuclear factor-kappaB activation and the production of

inflammatory cytokines in human endothelial cells. J Pharmacol Exp Ther 2008; 324: 103–110. [PubMed: 17947496]

19. Lakhkar A, Dhagia V, Joshi SR, Gotlinger K, Patel D, Sun D, Wolin MS, Schwartzman ML, Gupte SA. 20-HETE-induced mitochondrial superoxide production and inflammatory phenotype in vascular smooth muscle is prevented by glucose-6-phosphate dehydrogenase inhibition. Am J Physiol Heart Circ Physiol 2016; 310: H1107–1117. [PubMed: 26921441]
20. Kizub IV, Lakhkar A, Dhagia V, Joshi SR, Jiang H, Wolin MS, Falck JR, Koduru SR, Errabelli R, Jacobs ER, Schwartzman ML, Gupte SA. Involvement of gap junctions between smooth muscle cells in sustained hypoxic pulmonary vasoconstriction development: a potential role for 15-HETE and 20-HETE. Am J Physiol Lung Cell Mol Physiol 2016; 310: L772–783. [PubMed: 26895643]
21. Ran FA, Hsu PD, Wright J, Agarwala V, Scott DA, Zhang F. Genome engineering using the CRISPR-Cas9 system. Nat Protoc 2013; 8: 2281–2308. [PubMed: 24157548]
22. Schwenk F, Baron U, Rajewsky K. A cre-transgenic mouse strain for the ubiquitous deletion of loxP-flanked gene segments including deletion in germ cells. Nucleic Acids Res 1995; 23: 5080–5081. [PubMed: 8559668]
23. Stenmark KR, Meyrick B, Galie N, Mooi WJ, McMurtry IF. Animal models of pulmonary arterial hypertension: the hope for etiological discovery and pharmacological cure. Am J Physiol Lung Cell Mol Physiol 2009; 297: L1013–1032. [PubMed: 19748998]
24. Abe K, Toba M, Alzoubi A, Ito M, Fagan KA, Cool CD, Voelkel NF, McMurtry IF, Oka M. Formation of plexiform lesions in experimental severe pulmonary arterial hypertension. Circulation 2010; 121: 2747–2754. [PubMed: 20547927]
25. Hsia CC, Hyde DM, Ochs M, Weibel ER, Structure AEJTFoQAoL. An official research policy statement of the American Thoracic Society/European Respiratory Society: standards for quantitative assessment of lung structure. Am J Respir Crit Care Med 2010; 181: 394–418. [PubMed: 20130146]
26. Joshi SR, Kitagawa A, Jacob C, Hashimoto R, Dhagia V, Ramesh A, Zheng C, Zhang H, Jordan A, Waddell I, Leopold J, Hu CJ, McMurtry IF, D'Alessandro A, Stenmark KR, Gupte SA. Hypoxic activation of glucose-6-phosphate dehydrogenase controls the expression of genes involved in the pathogenesis of pulmonary hypertension through the regulation of DNA methylation. Am J Physiol Lung Cell Mol Physiol 2020; 318: L773–L786. [PubMed: 32159369]
27. Hashimoto R, Lanier GM, Dhagia V, Joshi SR, Jordan A, Waddell I, Tuder R, Stenmark KR, Wolin MS, McMurtry IF, Gupte SA. Pluripotent hematopoietic stem cells augment alpha-adrenergic receptor-mediated contraction of pulmonary artery and contribute to the pathogenesis of pulmonary hypertension. Am J Physiol Lung Cell Mol Physiol 2020; 318: L386–L401. [PubMed: 31913656]
28. El Kasmi KC, Pugliese SC, Riddle SR, Poth JM, Anderson AL, Frid MG, Li M, Pullamsetti SS, Savai R, Nagel MA, Fini MA, Graham BB, Tuder RM, Friedman JE, Eltzschig HK, Sokol RJ, Stenmark KR. Adventitial fibroblasts induce a distinct proinflammatory/profibrotic macrophage phenotype in pulmonary hypertension. J Immunol 2014; 193: 597–609. [PubMed: 24928992]
29. Pugliese SC, Poth JM, Fini MA, Olschewski A, El Kasmi KC, Stenmark KR. The role of inflammation in hypoxic pulmonary hypertension: from cellular mechanisms to clinical phenotypes. Am J Physiol Lung Cell Mol Physiol 2015; 308: L229–252. [PubMed: 25416383]
30. Maguire JJ, Jones KL, Kuc RE, Clarke MC, Bennett MR, Davenport AP. The CCR5 chemokine receptor mediates vasoconstriction and stimulates intimal hyperplasia in human vessels in vitro. Cardiovasc Res 2014; 101: 513–521. [PubMed: 24323316]
31. Iyinikkel JS. Identifying novel G protein-coupled receptor targets in pulmonary hypertension : uncovering the role of GPR75. Pharmacology. Aberdeen, UK: Institute of Medical Sciences; University of Aberdeen; 2018. p. 327.
32. McDonald DS. G protein-coupled receptor expression and function in Pulmonary Artery Smooth Muscle Cells : : Novel Targets in Pulmonary Arterial Hypertension. San Diego, USA: University of San Diego; 2013. p. 92.
33. Urban NH, Berg KM, Ratz PH. K+ depolarization induces RhoA kinase translocation to caveolae and Ca2+ sensitization of arterial muscle. Am J Physiol Cell Physiol 2003; 285: C1377–1385. [PubMed: 12890649]

34. Montani D, Chaumais MC, Guignabert C, Gunther S, Girerd B, Jais X, Algalarrondo V, Price LC, Savale L, Sitbon O, Simonneau G, Humbert M. Targeted therapies in pulmonary arterial hypertension. Pharmacol Ther 2014; 141: 172–191. [PubMed: 24134901]
35. Cahill E, Rowan SC, Sands M, Banahan M, Ryan D, Howell K, McLoughlin P. The pathophysiological basis of chronic hypoxic pulmonary hypertension in the mouse: vasoconstrictor and structural mechanisms contribute equally. Exp Physiol 2012; 97: 796–806. [PubMed: 22366565]
36. Manoury B, Idres S, Leblais V, Fischmeister R. Ion channels as effectors of cyclic nucleotide pathways: Functional relevance for arterial tone regulation. Pharmacol Ther 2020; 209: 107499. [PubMed: 32068004]
37. Suematsu E, Hirata M, Kuriyama H. Effects of cAMP- and cGMP-dependent protein kinases, and calmodulin on Ca2+ uptake by highly purified sarcolemmal vesicles of vascular smooth muscle. Biochim Biophys Acta 1984; 773: 83–90. [PubMed: 6329280]
38. Watras J Regulation of calcium uptake in bovine aortic sarcoplasmic reticulum by cyclic AMP-dependent protein kinase. J Mol Cell Cardiol 1988; 20: 711–723. [PubMed: 3221409]
39. Endou K, Iizuka K, Yoshii A, Tsukagoshi H, Ishizuka T, Dobashi K, Nakazawa T, Mori M. 8-Bromo-cAMP decreases the Ca2+ sensitivity of airway smooth muscle contraction through a mechanism distinct from inhibition of Rho-kinase. Am J Physiol Lung Cell Mol Physiol 2004; 287: L641–648. [PubMed: 15121638]
40. Nagaoka T, Gebb SA, Karoor V, Homma N, Morris KG, McMurtry IF, Oka M. Involvement of RhoA/Rho kinase signaling in pulmonary hypertension of the fawn-hooded rat. J Appl Physiol (1985) 2006; 100: 996–1002. [PubMed: 16322374]
41. Jones C, Bisserier M, Bueno-Beti C, Bonnet G, Neves-Zaph S, Lee SY, Milara J, Dorfmuller P, Humbert M, Leopold JA, Hadri L, Hajjar RJ, Sassi Y. A novel secreted-cAMP pathway inhibits pulmonary hypertension via a feed-forward mechanism. Cardiovasc Res 2020; 116: 1500–1513. [PubMed: 31529026]
42. Kimura TE, Duggirala A, Smith MC, White S, Sala-Newby GB, Newby AC, Bond M. The Hippo pathway mediates inhibition of vascular smooth muscle cell proliferation by cAMP. J Mol Cell Cardiol 2016; 90: 1–10. [PubMed: 26625714]
43. Klemm DJ, Watson PA, Frid MG, Dempsey EC, Schaack J, Colton LA, Nesterova A, Stenmark KR, Reusch JE. cAMP response element-binding protein content is a molecular determinant of smooth muscle cell proliferation and migration. J Biol Chem 2001; 276: 46132–46141. [PubMed: 11560924]
44. Abe K, Shinoda M, Tanaka M, Kuwabara Y, Yoshida K, Hirooka Y, McMurtry IF, Oka M, Sunagawa K. Haemodynamic unloading reverses occlusive vascular lesions in severe pulmonary hypertension. Cardiovasc Res 2016; 111: 16–25. [PubMed: 27037259]
45. Lv D, Zhang Y, Kim HJ, Zhang L, Ma X. CCL5 as a potential immunotherapeutic target in triple-negative breast cancer. Cell Mol Immunol 2013; 10: 303–310. [PubMed: 23376885]
46. Ammit AJ, Hoffman RK, Amrani Y, Lazaar AL, Hay DW, Torphy TJ, Penn RB, Panettieri RA Jr. Tumor necrosis factor-alpha-induced secretion of RANTES and interleukin-6 from human airway smooth-muscle cells. Modulation by cyclic adenosine monophosphate. Am J Respir Cell Mol Biol 2000; 23: 794–802. [PubMed: 11104733]
47. Hallsworth MP, Twort CH, Lee TH, Hirst SJ. beta(2)-adrenoceptor agonists inhibit release of eosinophil-activating cytokines from human airway smooth muscle cells. Br J Pharmacol 2001; 132: 729–741. [PubMed: 11159726]
48. Garat CV, Majka SM, Sullivan TM, Crossno JT Jr., Reusch JEB, Klemm DJ. CREB depletion in smooth muscle cells promotes medial thickening, adventitial fibrosis and elicits pulmonary hypertension. Pulm Circ 2020; 10: 2045894019898374. [PubMed: 32313640]
49. Zhang F, Wang MH, Wang JS, Zand B, Gopal VR, Falck JR, Laniado-Schwartzman M, Nasjletti A. Transfection of CYP4A1 cDNA decreases diameter and increases responsiveness of gracilis muscle arterioles to constrictor stimuli. Am J Physiol Heart Circ Physiol 2004; 287: H1089–1095. [PubMed: 15130884]

50. Zhu D, Birks EK, Dawson CA, Patel M, Falck JR, Presberg K, Roman RJ, Jacobs ER. Hypoxic pulmonary vasoconstriction is modified by P-450 metabolites. Am J Physiol Heart Circ Physiol 2000; 279: H1526–1533. [PubMed: 11009437]

51. Dunham-Snary KJ, Wu D, Sykes EA, Thakrar A, Parlow LRG, Mewburn JD, Parlow JL, Archer SL. Hypoxic Pulmonary Vasoconstriction: From Molecular Mechanisms to Medicine. Chest 2017; 151: 181–192. [PubMed: 27645688]

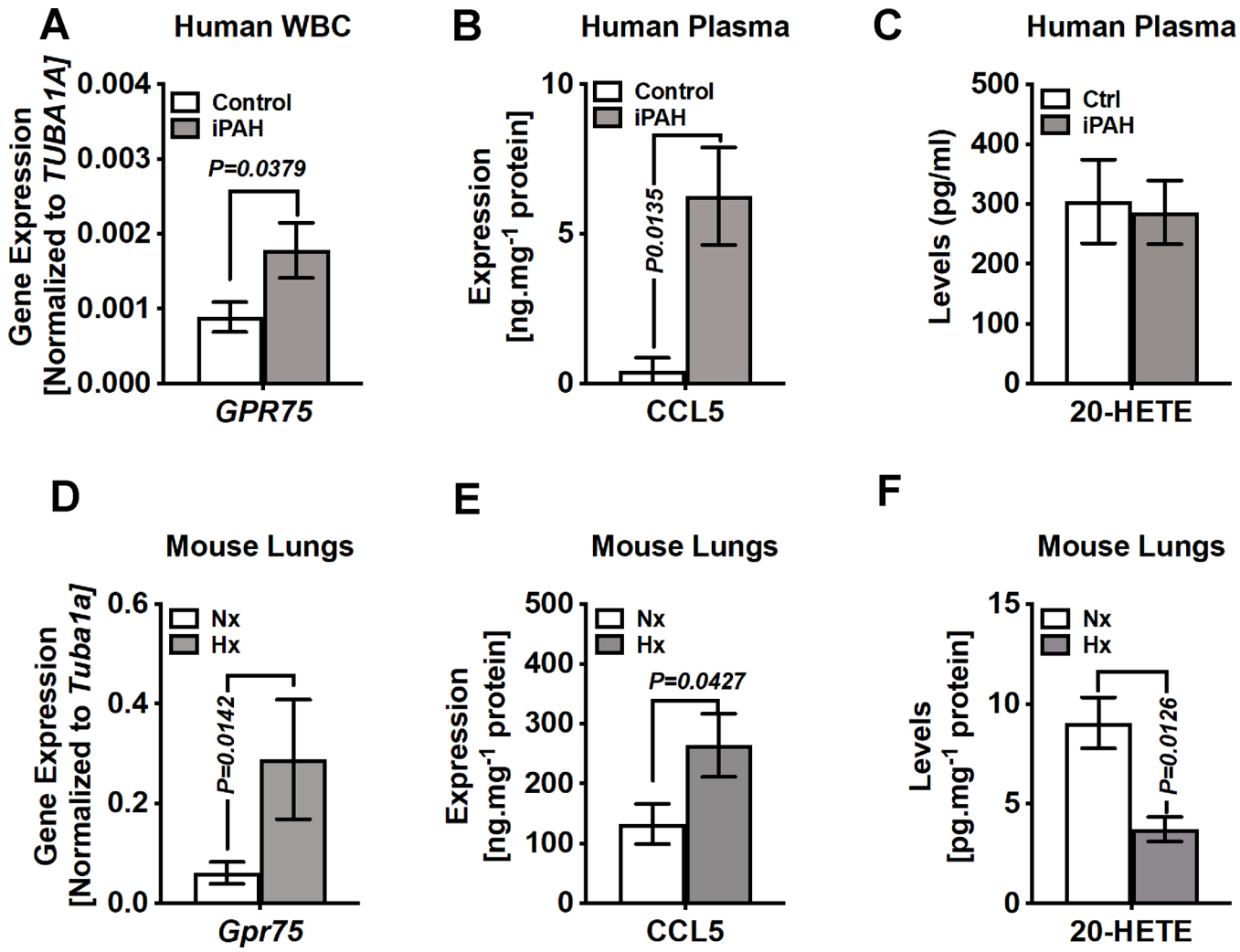

Figure 1: GPR75 mRNA and CCL5 protein are increased in PH.

(A-C) Levels of GRP75 mRNA and CCL5 protein are higher in white blood cells and plasma from idiopathic PH patients (N=6; and sex: F) than control individuals (N=6; and sex: F). 20-HETE levels do not differ between the two groups. (D-F) GRP75 mRNA and CCL5 protein expression are higher, while 20-HETE levels are lower, in lungs from female wild-type mice exposed to hypoxia (Hx; N=5) than in those exposed to normoxia (Nx; N=5). Statistical comparisons were made with Student's *t*-test.

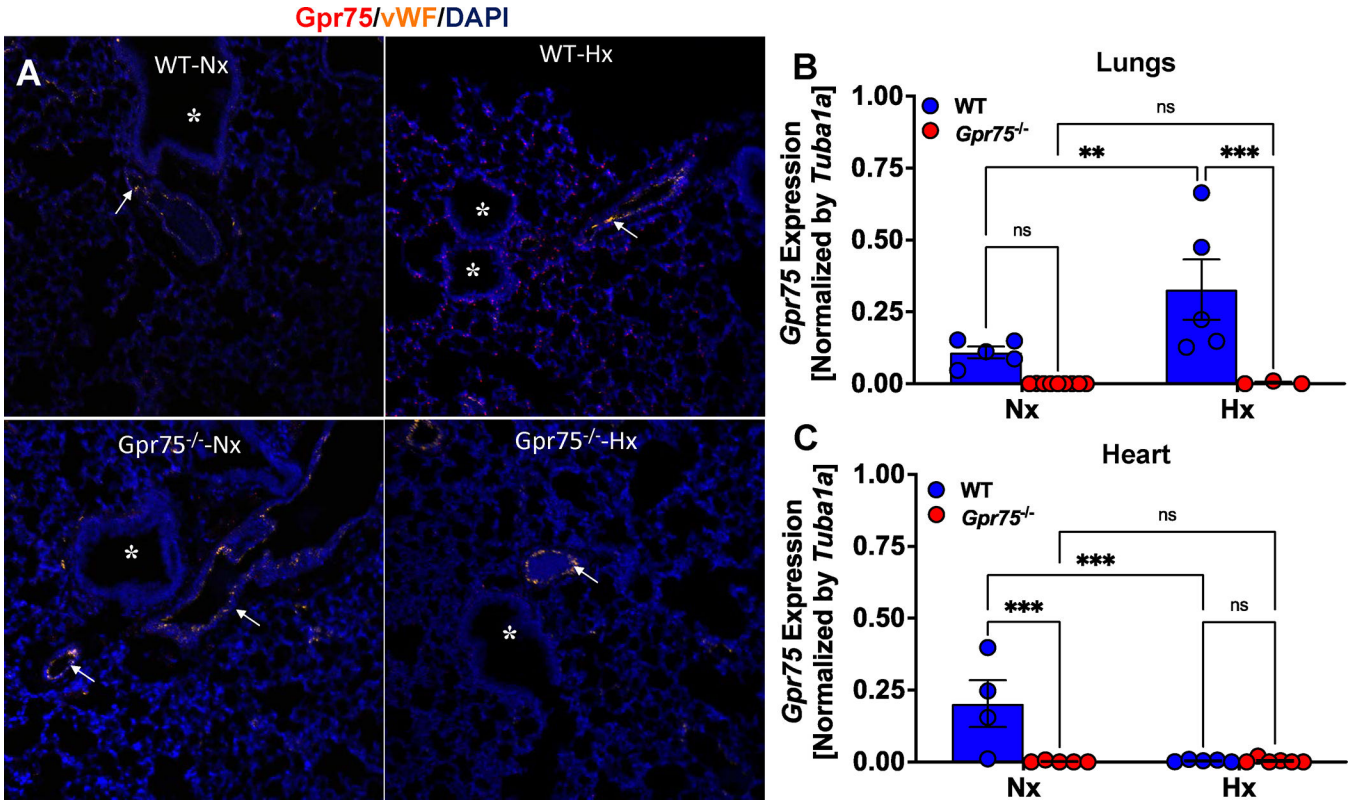

Figure 2: *Gpr75* expression is increased in lungs of mice exposed to hypoxia.

(A) Representative micrographs from three different experiments using RNAscope™ probes for *in situ* hybridization of *Gpr75* (red) and *wVF* (yellow/orange indicated by arrow) in lungs of normoxic and hypoxic (5 weeks) wild-type and *Gpr75*$^{-/-}$ mice. Nuclei are stained with DAPI (blue). Magnification: 20x. Arrows indicate pulmonary arteries, asterisks the airways. (B, C) qPCR results showing that *Gpr75* mRNA levels were increased in lungs and decreased in hearts from wild-type (WT) mice, but not *Gpr75* knockout mice (*Gpr75*$^{-/-}$), exposed to hypoxia (Hx). Statistical comparisons were made with two-way ANOVA followed by Fisher's LSD post hoc test. **P*<*0.05* and ***P*<*0.005*.

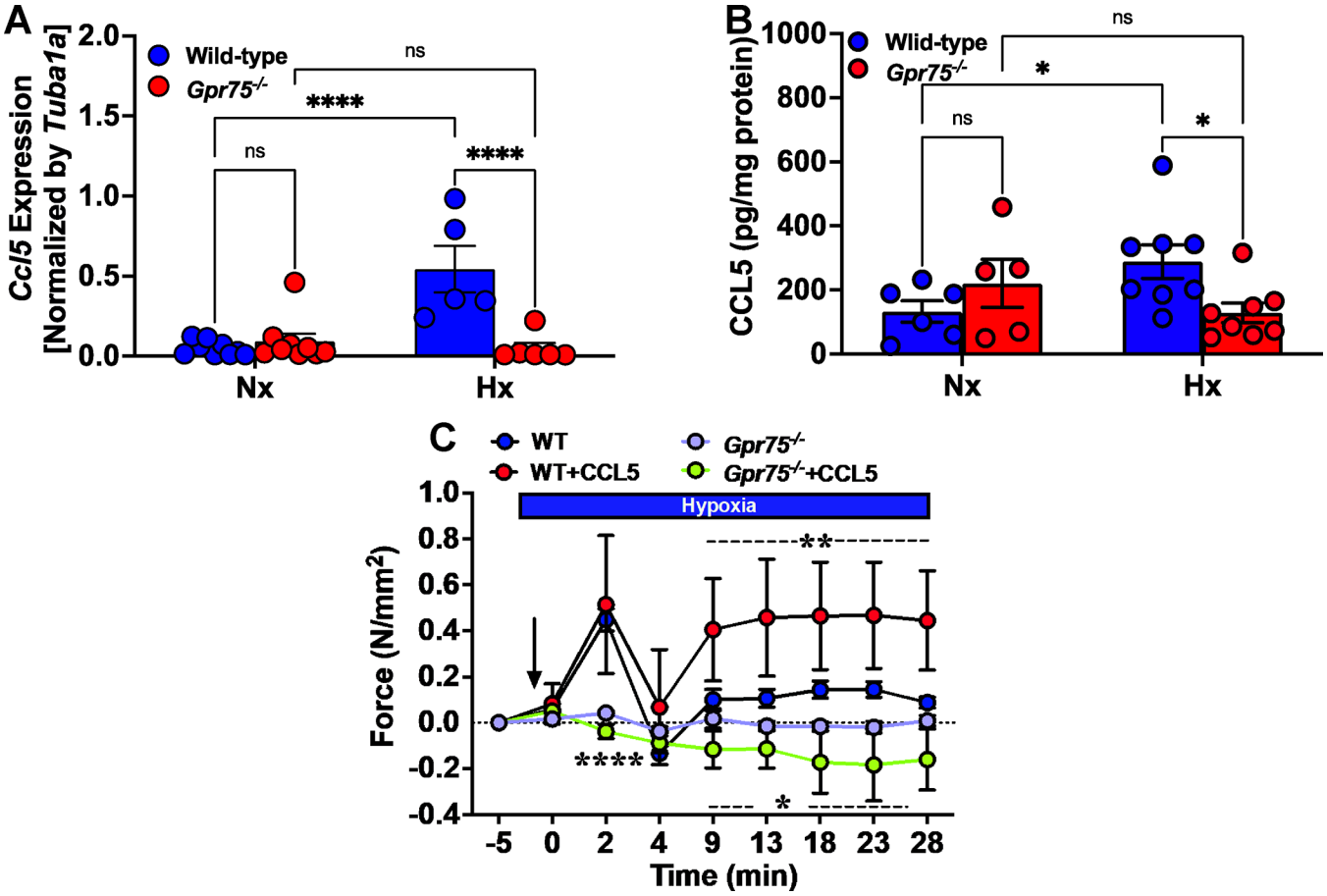

Figure 3: Increased CCL5 in lungs of wild-type mice exposed to hypoxia augments hypoxia-induced contractions in intralobar pulmonary arteries.

(A and B) Expression of CCL5 mRNA and protein was higher in lungs from WT Hx mice than Nx mice, but there was no difference between *Gpr75*$^{-/-}$-Hx and Nx mice. (C and D) Hypoxia-induced contractions of intralobar pulmonary arteries (IPAs) from *Gpr75*$^{-/-}$ mice were weaker than those in IPAs from WT mice (Po_2=40 Torr). Both the first and second phases of hypoxia-induced pulmonary artery contractions are weaker in *Gpr75*$^{-/-}$ than WT mice. IPA rings from *Gpr75*$^{-/-}$ and WT mice were precontracted with phenylephrine (1 μmol/L) and had similar baseline tones prior to exposure to hypoxia. Notably, CCL5 (1 ng/ml) augmented the second phase of hypoxic contractions. Statistical comparisons were made with two-way ANOVA followed by Fisher's LSD post hoc test. N=40 in the WT control group; N=16 in the *Gpr75*$^{-/-}$ control group; N=6 in the WT CCL5/20-HETE group; N=5 in the *Gpr75*$^{-/-}$ CCL5/20-HETE group (Panel C). *$P<0.05$, **$P<0.005$, and ****$P<0.0005$.

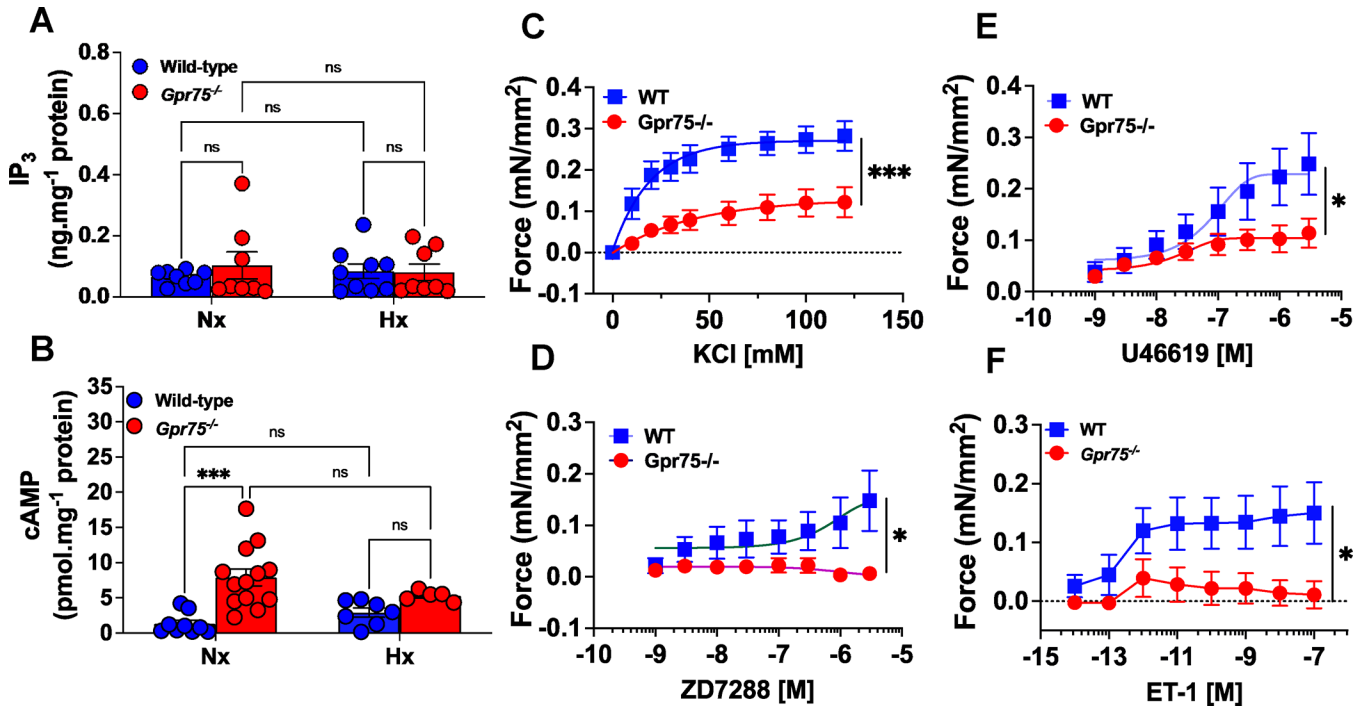

Figure 4: *Gpr75* knockout increases cAMP and decreases IPA contractions elicited by various contractile agents.

(A) Inositol 1,3,5-triphosphate (IP3) levels in the lungs of *Gpr75*$^{-/-}$ and WT mice do not differ between those in the Hx and Nx groups. (B) cAMP levels are higher in lungs from *Gpr75*$^{-/-}$ than WT mice. Application of (C) KCl, (D) ZD7288, (E) U46619 or (F) endothelin-1 (ET-1) to IPAs from WT and *Gpr75*$^{-/-}$ mice elicited contraction in a dose-dependent manner. Contractions were stronger in IPAs from WT than *Gpr75*$^{-/-}$ mice. Statistical comparisons were made with two-way ANOVA followed by Fisher's LSD post hoc test. **P*<*0.05,* ****P*<*0.001.* N=8 in wild-type and N=12 in *Gpr75*$^{-/-}$ group (Panels C to F).

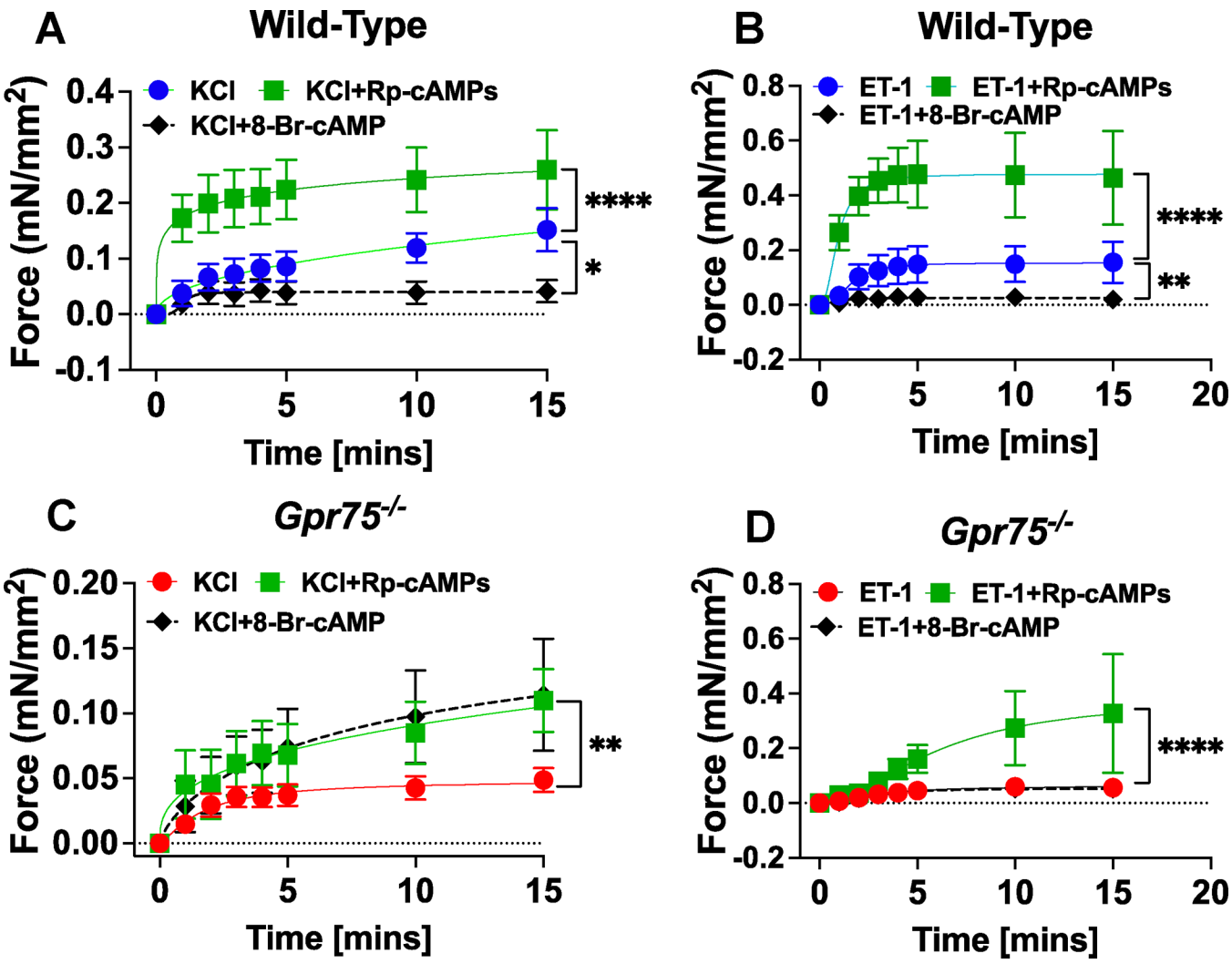

Figure 5: Effect of a PKA activator and inhibitor on KCl- and endothelin-1-evoked contractions in IPAs from wild-type and *Gpr75*$^{-/-}$ mice.

IPAs from wild-type (A, B) and *Gpr75*$^{-/-}$ (C, D) mice were pretreated for 10 min with 8-Br-cAMP, a PKA activator, or with Rp-cAMPs, a PKA inhibitor, before applying KCl (60 mM) or endothelin-1 (1 μM). Force generation was recorded with wire myography. (A, B) Pretreatment with 8-Br-cAMP or Rp-cAMPs respectively decreased or increased KCl- and endothelin-1-evoked contractions in IPAs from wild-type mice. (C) Pretreatment with 8-Br-cAMP did not decrease KCl- or endothelin-1-evoked IPA contractions in *Gpr75*$^{-/-}$ mice. (D) Unlike with IPAs from wild-type mice, Rp-cAMPs gradually enhanced KCl- and endothelin-1-evoked contractions in IPAs from *Gpr75*$^{-/-}$ mice. In panel D, control and 8-Br-cAMP curves overlap. Statistical comparisons were made with two-way ANOVA followed by Fisher's LSD post hoc test. *$P<0.05$, **$P<0.005$, and ****$P<0.0001$. N=5 in the wild-type group; N=13 in the *Gpr75*$^{-/-}$ control group and N=6 in the *Gpr75*$^{-/-}$-treated groups.

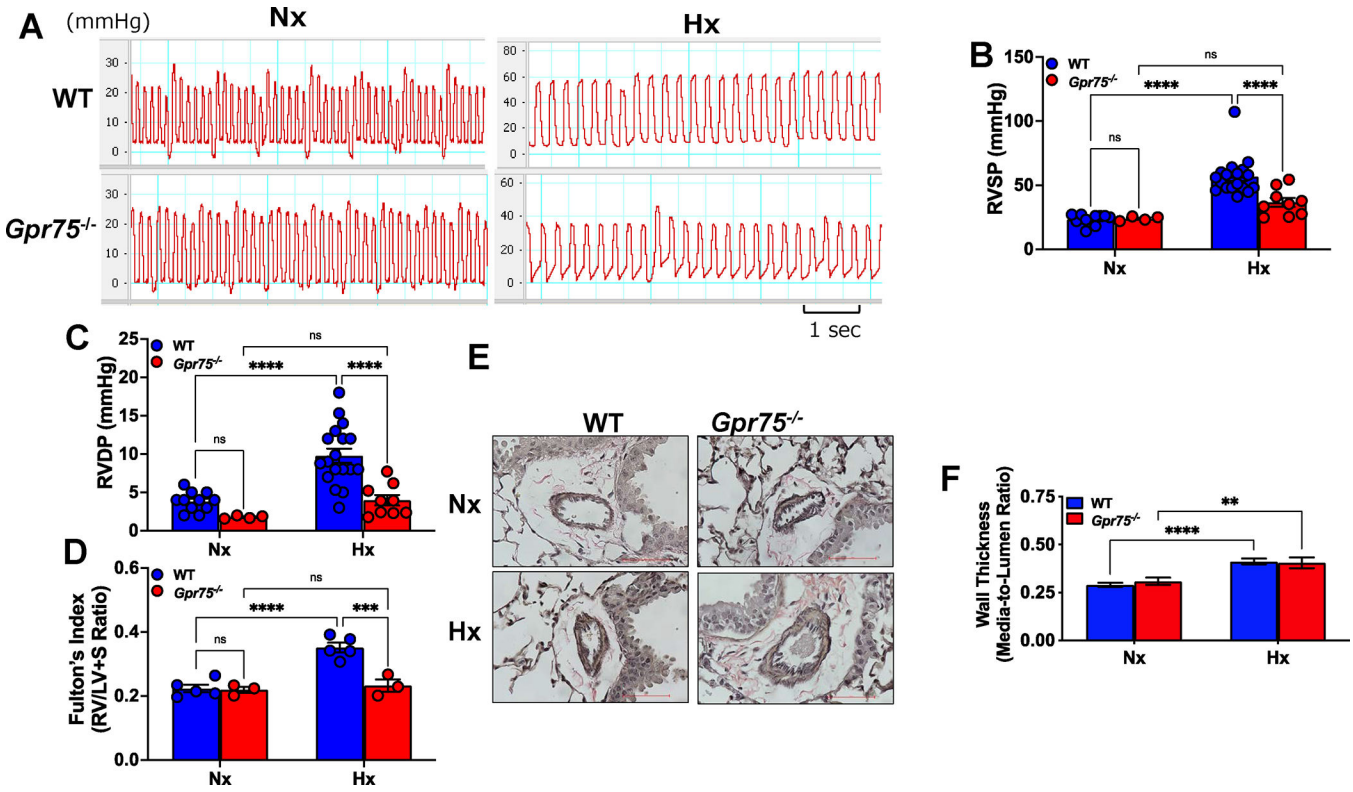

Figure 6: Global *Gpr75* knockout decreases hypoxia-induced PH.

(A) Representative traces show right ventricular pressure recorded by inserting a pressure catheter into the right heart of *Gpr75*$^{-/-}$ and WT mice. (B, C) Right ventricular systolic (RVSP) and diastolic (RVDP) pressures increased in WT but not *Gpr75*$^{-/-}$ mice. (D) Right ventricular hypertrophy (Fulton's Index) increased in WT but not *Gpr75*$^{-/-}$ mice. (E) Pulmonary arterial wall thickness (hypertrophy) increased in WT and *Gpr75*$^{-/-}$ mice. Statistical comparisons were made with two-way ANOVA followed by Fisher's LSD post hoc test. $^{**}P<0.005$, $^{**}P<0.001$, and $^{****}P<0.0001$. Average wall thicknesses of approximately 200–300 pulmonary arteries (100 μm) counted in five WT and *Gpr75*$^{-/-}$ mice are shown (Panel F).

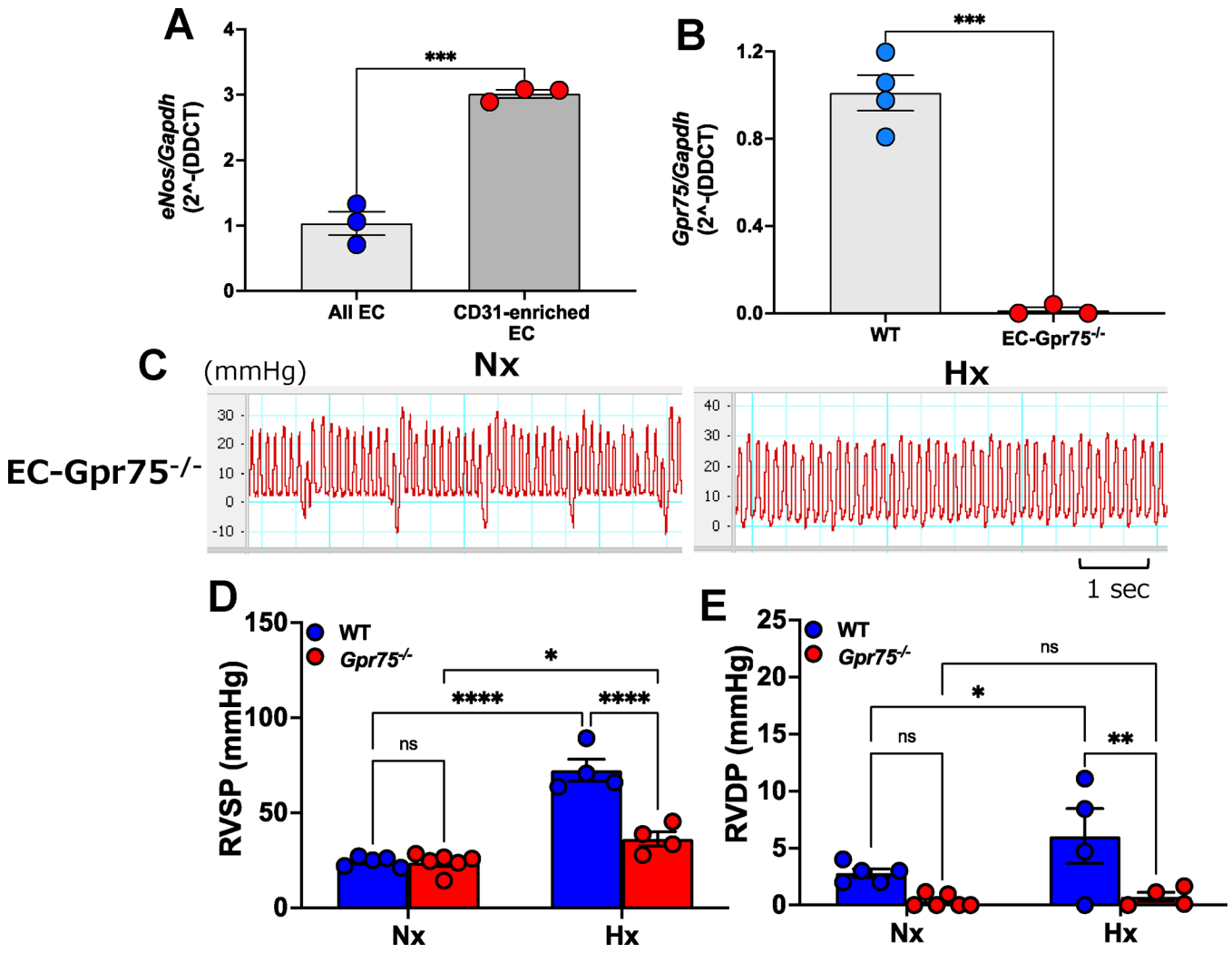

Figure 7: EC *Gpr75* knockout decreases hypoxia-induced PH.

A) Enrichment of ECs isolated from lungs, as measured based on *eNos* expression with bead-sorted CD31-conjugated Dynabeads. B) *Gpr75* expression in CD31-sorted ECs from lungs of WT (Tie-Cre) and EC *Gpr75* knockout mice (*EC-Gpr75*$^{-/-}$). (C) Right ventricular pressure was recorded in EC-*Gpr75*$^{-/-}$ mice exposed to normobaric hypoxia (Hx; 10% O_2) or normoxia (Nx) for 5 weeks. (D, E) Right ventricular systolic (RVSP) and diastolic (RVDP) pressures were increased in WT and EC-*Gpr75*$^{-/-}$ mice but to a lesser degree in EC-*Gpr75*$^{-/-}$ mice than WT mice. Statistical comparisons were performed with two-way ANOVA followed by Fisher's LSD post hoc test. ** *P<0.005*, ** *P<0.001* and **** *P<0.0001.*